Fabrication of large-area face-centered-cubic hard-sphere colloidal crystals by shear alignment

R. M. Amos,* J. G. Rarity, P. R. Tapster, and T. J. Shepherd
DERA, St. Andrews Road, Malvern, Worcestershire WR14 3PS, United Kingdom

S. C. Kitson
Hewlett Packard Laboratories, Bristol, United Kingdom

(Received 24 May 1999; revised manuscript received 2 November 1999)

We make hard-sphere colloidal crystals from polymethyl methacrylate spheres suspended in organic solvents at high volume fractions. The samples are crystallized between two glass plates separated by 10-μm spacer beads. We study the optical scattering from these systems and describe methods for discriminating between the various crystal packings. Crystals formed simply by increasing the volume fraction beyond the liquid-solid phase transition tend to be small and predominantly random close packed. However, we find that by forming these crystals while applying controlled shear to the glass plates, large-area single crystals can be made. These crystals are much more regular and appear to be predominantly twinned face-centred cubic. The creation of single-orientation face-centred cubic crystals appears possible when shear is applied in one direction.

PACS number(s): 82.70.Dd, 42.70.Qs

INTRODUCTION

There is currently much interest in materials that possess a periodic modulation in refractive index at optical wavelength scales. Such materials exhibit stop bands in their transmission at certain well-defined frequencies dictated by the periodicity, direction of propagation, and polarization. Extending the periodicity to three dimensions and by suitably increasing the dielectric contrast opens the prospect of creating a material wherein all electromagnetic propagation is disallowed for a range of optical frequencies [1,2]. This is known as a photonic band gap (PBG) material. Within the band gap the optical density of states is zero. Purcell [3] was the first to propose that spontaneous emission can be modified by controlling the density of states; PBG materials have enormous potential in improving laser cavity design greatly reducing threshold and increasing efficiency. Indeed the vertical cavity surface emitting laser is an example of a structure that exploits a one-dimensional periodic modulation in index to define the lasing cavity [4].

The formation of a photonic band gap depends on the detailed periodic structure of the material. Structures based on the face-centred cubic (fcc) unit cell have a near-spherical Brillouin zone and are good candidates for producing a wide band gap [5]. Breaking the periodicity (for example, by the introduction of defects into the structure) can modify the optical properties and create localized modes. This has recently been realized in a two-dimensional (2D) periodic optical fiber in which light propagates down a central defect [6]. However, materials which possess a full photonic band gap at optical wavelengths have yet to be demonstrated experimentally as a result of the difficulty in fabrication and achieving the required refractive index contrast.

Nevertheless, there have been a number of successful approaches in producing 3D periodic materials which show partial gaps in the optical regime [7–10]. Photolithographic and etching techniques can create 3D periodicity in semiconductor materials with periods of a few μm, but to date have been limited to just a few periods deep [11]. A much faster and larger area fabrication technique is to interfere four laser beams in a photosensitive film [12]. The exposed regions of the film are rendered insoluble and development results in a 3D periodic network of resin and air. The air gaps can then be filled with a material of high refractive index (for example, TiO_2). An alternative approach has been to use colloidal crystals—these are small wavelength-scale dielectric spheres that under the right conditions self-assemble into a 3D lattice similar to that of an atomic lattice [13].

The formation of optical-scale hard-sphere crystals from monodisperse colloidal dispersions has been studied for some time. Such systems have proved extremely useful models for studies of the liquid-solid-glass phase transition [14,15]. There are a number of methods of producing colloidal crystals. One is to suspend charged spheres (such as polystyrene) in a liquid at low volume concentrations. Electrostatic forces push the spheres apart to form a crystalline lattice, the period of which can be controlled by the pH of the liquid (the charge on the spheres) and the sphere diameter. Body-centered cubic (bcc) and fcc crystals have been demonstrated [16–18]. Another method is the sedimentation of hard, close-packed spheres in a liquid. Crystallization occurs over a period of days or weeks depending on the sedimentation rate. Synthetic opals can be fabricated by the sedimentation of silica spheres suspended in a liquid. The liquid can be evaporated and the resulting dry crystal infiltrated with other materials to increase the refractive index contrast [19,20]. Alternatively, the dry silica crystal can be heated (sintered) to fuse the spheres together. After infiltration with another material (such as TiO_2) the silica spheres can be removed by dissolving in acid, thus forming the inverse crystal structure [21–23]. Uniform fcc crystals of silica spheres have also been formed by sedimentation onto a square template [24].

*Electronic address: Ramos@dera.gov.uk

It has also been shown that for a hard sphere, interaction potential spontaneous crystallization can occur depending on the volume concentration [14,15]. For volume fractions $f > 0.49$ a polycrystalline phase separates from the initially liquidlike structure. The crystalline phase fills the entire sample when f reaches 0.54 and glassy states form for $f > 0.58$. In initial light scattering experiments the scattered intensity from many crystallites was studied as a function of angle [25]. This is equivalent to the well-known x-ray powder diffraction method, and study of the detailed structure of the Bragg ring allows the structure within the crystallites to be deduced. It was concluded that the crystalline phase was primarily made up of small (100 μm) crystallites with primarily random close-packed (RCP) structure consisting of a random stacking of hexagonally close-packed (HCP) layers.

The methods discussed above are slow (sedimentation takes many days or weeks to form colloidal crystals) and tend to create small crystallites. There is no control over the dimensions of the crystal, its orientation or structure, and perhaps most importantly there is no control over the defect density. Recent experiments [26,27] have shown that shearing along one direction during crystallization increases the size of the crystallites and can induce the formation of millimeter-sized fcc crystals. The shear was induced by rocking the cuvette containing the crystallizing sample which induces flow. As a result the amount of shear varies throughout the cell leading to various crystalline structures in different regions of the sample. Similar variable structured large crystals were obtained in a crystallization experiment carried out in zero-gravity conditions [28,29]. Recently, shear-induced order has been reported for triblock copolymers in solution in a cylindrical geometry [30]. Miscelles of 6-nm diameter are formed which align into HCP planes under steady shear and twinned fcc structures under oscillatory shear. The structure was characterized by small-angle neutron scattering. Shear has also been applied by suspending a colloidal crystal between two parallel plates [31–35]. It was shown that under high strain conditions HCP layers of spheres formed aligned parallel with the flow direction. Application of low strain produced a polycrystalline structure consisting of HCP planes aligned perpendicular to the shear direction. Local disorder was observed using optical microscopy revealing dislocations, vacancies, and stacking faults.

In the experiments reported here we study a similar geometry, that of hard sphere crystals confined between two glass plates separated by about 10μm. We use polymethyl methacrylate (PMMA) spheres stabilized by a thin layer of grafted polymer (poly-12-hydroxystearate) and suspended in either dodecane or octanol. We find that at volume fractions around $f = 0.53$, crystals form across most of the sample in seconds, essentially growing from the walls as HCP planes. The crystallite size is small—typically 100 μm in the plane of the cell. Illuminating with a weakly focused laser normal to the cell leads to a sixfold Bragg spot pattern typical of RCP crystallites. However, this simple pattern does not uniquely characterize the structure as there is also a weak powderlike ring linking the six spots. This could arise simply from a single HCP layer at either glass surface with a frozen liquidlike structure between. To characterize fully the sample we alter the angle of incidence of the laser and study the evolution of the intensities in the spots. In this way we have been able to confirm the 3D RCP nature of the structure. However, in small areas of some samples we are able to identify regions where a fcc structure predominates. Here the sixfold spot pattern is divided into two sets of three spots with differing brightness with 100% fcc characterized by a single set of three spots.

These thin cells are ideal for applying uniform and controlled shear during crystallization simply by sliding one glass plate with respect to the other [31,32]. We are able to monitor the crystal size by watching the diffraction colors produced by white light illumination and the local structure by studying the laser-induced diffraction spots at intervals during the shearing process. Using an oscillating ($\sim$0.5 Hz) displacement of $\sim$0.1 mm disrupts the local crystal order during shear, but a few seconds after ceasing oscillation the assembly recrystallizes with larger crystallites. In this way we are able to produce a single crystal region spanning the entire area of the cell ($\sim$2 cm^2). Under laser illumination the structure produces a strong sixfold scattering pattern without any diffuse ring, indicating good local ordering throughout the cell. Although the six-spot pattern suggests that we still have random close packing of the layers, careful study of the evolution of the patterns with laser angle of incidence reveals that the structure is actually twinned fcc, similar to the results for triblock copolymer miscelles [26,30]. We suspect that the two fcc regions are associated with the top and bottom surfaces of the cell.

To investigate this further we apply a small amount of shear comparable with that required to shift the structure by one lattice spacing per layer ($\sim$10 μm). Illumination during the application of a small amount of shear reveals that the structure can be switched between the two forms of fcc. We first describe the fabrication and characterization of shear-ordered PMMA crystals dispersed in octanol, and continue with a brief description of the theory used to compare to experiment from which we deduce the 3D ordering within the crystal. We conclude with transmission data for two twinned fcc crystals that show a partial band gap at 1941 nm.

EXPERIMENTAL PROCEDURE

We use concentrated suspensions of 790-nm-diameter PMMA spheres stabilized by poly-12-hydroxystearate [36]. A suspension of spheres was washed in octanol several times and dried. A portion of these spheres was mixed with octanol

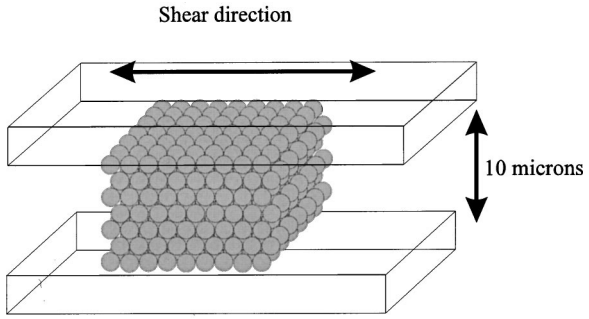

FIG. 1. The cell geometry used for the shear alignment of colloidal crystals. Two glass slides are separated by spacer beads and filled with a colloidal suspension of 790-nm-diameter PMMA spheres dispersed in octanol.

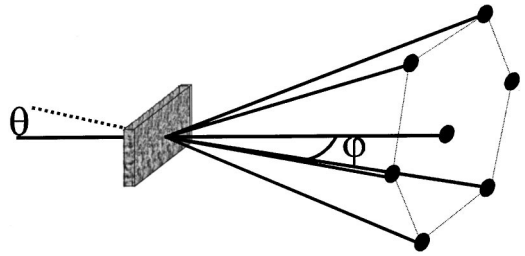

FIG. 2. The experimental arrangement used to characterize the colloidal crystal structure. Not shown is the cylindrical bowl of deionized water in which the sample was immersed so that higher-order diffracted spots can be measured. Typical experimental data are shown in Fig. 4. θ denotes the angle between the incident laser beam and the normal to the sample face, and φ is the scattered angle measured with respect to the transmitted beam as shown.

in a clean bottle to produce a standard stock solution of volume concentration 53%. It has been shown that for a hard sphere interaction potential between neighboring spheres, spontaneous crystallization occurs for concentrations from 49 to 54% [14,15,25]. We have independently verified this dependence by studying the crystallization in dodecane.

Two glass slides were cleaned and cut to size. Polystyrene spacer beads of 10-μm diameter were spread sparingly onto one of the slides to control the thickness of the assembled cell. A small amount of colloidal suspension was placed on the largest slide and the other placed on top, Fig. 1. At this point capillary action caused the colloidal suspension to fill the entire cell over a period of minutes. By studying the cell with a white light source iridescence could gradually be seen, indicating the formation of crystals. The domains sizes were small, of the order of a few 100 μm and their orientation was RCP, as determined by light scattering experiments described in the next section.

The crystal growth was characterized as a function of the volume concentration from 49 to 54% (dodecane was used for this study). It was found that below 49% volume concentration crystals would not form and the cell looked milky, indicating random scattering of the white light. This corresponds to a fluidlike structure. From 50 to 54% volume concentration crystals could be observed around the edges of the cell, first at 50%, and filling the entire cell at 54%. We observed Bragg scattering from these cells by illuminating normal to the sample with a laser beam (of wavelength 476 nm) and projecting the diffraction pattern onto a screen a few centimeters from the cell, Fig. 2. For the 49% volume concentration sample the diffraction pattern consisted of a ring. The angle at which the ring emerged indicated a fluidlike structure of nearly touching spheres of diameter 790 nm. For the higher concentrations the ring split into many bright spots, indicating the presence of many small crystals with different orientations present in the illumination region. For small regions in the highest concentration cell this ring reduced to just six spots, indicating the presence of a single crystal with hexagonally packed spheres in planes parallel to the glass slides. As the beam was moved around the sample, distinct crystal domains were evident as a rotation of the six spots, indicating a difference in crystal domain orientation with respect to the laser beam.

In order to align and increase the domain size we introduced a shearing force by moving the bottom glass slide with respect to the top. This was achieved by attaching the bottom slide to a linear translation stage and the top slide to a post fixed to the optical table. A probe laser beam was made incident normal to the sample from below so that the Bragg spots from the colloidal sample could be monitored during the shearing process. It is well known that colloidal crystals are weakly bound and a relatively small force can induce melting. Melting was observed by applying a large-scale shear. The bottom slide was moved backwards and forwards by a distance of about 0.1 mm and at a frequency of about 0.5 Hz. The scattered light intensity pattern changed from six spots to a continuous ring indicating that melting had occurred, producing a fluidlike state. When the shear was removed recrystallization occurred over a period of several seconds and the six Bragg spot pattern was recovered. Importantly, in contrast to the case before the shearing force had been applied, the six Bragg spots were evident from across the entire cell (i.e., no rotation or movement as the laser beam transversed the cell) indicating long-range order parallel to the glass slide walls.

To control the ordering in the direction perpendicular to the glass slides we used the same linear shear (same direction backwards and forwards) but reduced the extent of the translation to 10 μm equivalent to one lattice constant per layer in the crystals. Immediately, the Bragg spot pattern changed as we applied the shear, Fig. 3. On the forward stroke of the translation three of the six Bragg spots separated by 120°

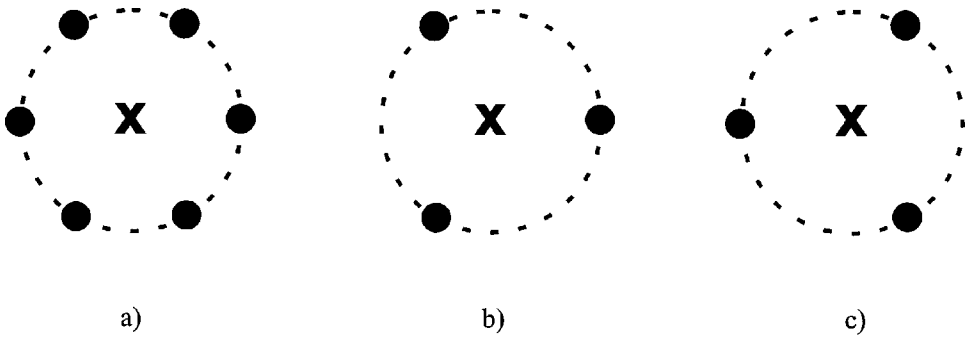

FIG. 3. Schematic of the experimentally observed Bragg diffraction spots from a shear aligned colloidal crystal. (a) could represent a RCP structure or a twinned fcc structure. (b) shows the pattern observed from one fcc stacking sequence and (c) from the other fcc stacking sequence, which are observed as the shearing force is applied. The dotted line shows the position of the powder diffraction ring, *X* marks the transmitted beam.

increased in intensity, while the other three Bragg spots decreased in intensity. Conversely, on the backward stroke the first set of spots decreased in intensity while the second set increased in intensity. This implies that the stacking sequence of the hexagonal layers is different for the two directions of shear. In the following section we give evidence supporting the notion that the stacking sequence corresponds to two forms of a fcc structure.

CHARACTERIZATION

After the shearing process was complete, the cell was sealed with an epoxy resin to ruggedize the crystal and to prevent evaporation of the octanol. After the resin had hardened the crystal produced six Bragg spots over the entire area of the cell, an indication that the long-range order is maintained parallel to the glass slides. In general we were unable to make large-area crystals showing just three Bragg spots with a linear shear; the crystals tend to relax into a six Bragg spots configuration over a period of minutes as the glue dried [26]. We attribute this change to relaxation processes after the shearing (residual movement in the apparatus and thermal movement of the spheres). The resultant crystal structure is actually twinned fcc, with both configurations coexisting in the same region of the sample. Similar results have been observed when oscillatory shear is applied to triblock copolymers [30]. We have confirmed the twinned fcc structure by optical characterization.

The intensity of the six Bragg spots was first measured as a function of the incident angle θ between the laser beam and the normal to the glass slides. This is schematically shown in Fig. 2. The sample was placed at the center of a cylindrical glass bowl filled with deionized water, so that higher-order Bragg spots could be observed. It was mounted on a stage allowing rotation around all three orthogonal axes, so that the center of rotation was coincident with the laser beam. A detector was placed on an arm attached to a rotation stage with its center coincident with the illuminated region of the sample. The sample was rotated around an axis parallel to the laser beam so that two of the six Bragg spots were horizontal. We note that the angle at which the Bragg spots are observed can be analyzed by considering each layer within the colloidal crystal as a 2D diffraction grating. The pitch of the grating is equal to $d\sqrt{3}/2$ where d is the effective sphere diameter. Following simple diffraction theory we can write

$$\sin\theta + \sin(\theta - \phi) = \frac{\lambda_0}{n\lambda_G},$$

where θ is the angle of incidence, ϕ is the angle of the diffracted Bragg spot beam measured from the zero-order transmitted beam, n is the refractive index of the water, λ_0 the incident wavelength, and λ_G the grating pitch. Thus if we plot $\sin\theta$ against $\sin(\theta-\phi)$ we obtain a linear dependence with a gradient of -1 and an intercept of $\lambda_0/n\lambda_G$, see Fig. 4. From this we can deduce the sphere size to be 790 nm if we assume that the spheres are touching.

The angle of incidence was set at some known value and the detector rotated to sweep through the spots. Typical data are shown in Fig. 5. The intensity at zero degrees ($\varphi = 0$) corresponds to the intense zero-order transmitted beam which overloaded the detector. The Bragg spots are clearly evident at $\pm 32.8°$ for this particular angle of incidence ($\theta = 0$). An estimate of the relative intensity of the Bragg spot was obtained by integrating the area under the peak. The angle of incidence was then changed and the measurement repeated. The result showing Bragg spot intensity as a function of incidence angle is shown in Fig. 6. To understand this dependence we compared the experimental result with that generated by a simple scattering theory, which we describe in the following section.

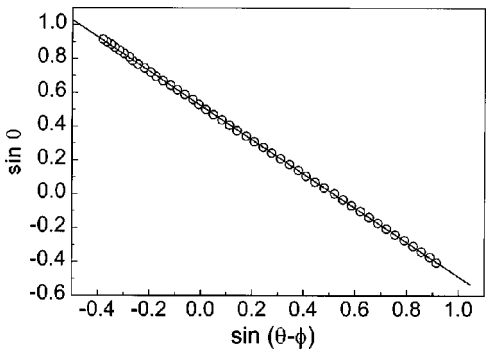

FIG. 4. The angular dependence of the diffracted beams from the colloidal sample as a function of the angle of incidence. The solid line is a linear fit to the data from which the sphere size can be determined as 790 nm.

THEORETICAL MODELING

A simple theory has been developed to model the light scattering properties of shear aligned colloidal crystals. A typical sample consists of a thin layer of the colloid confined between glass plates. It is thus safe to assume that the colloid can be represented as a few layers, where each layer is a single sheet of closely packed spheres in a hexagonal arrangement. Successive layers are then stacked to form a close-packed structure. This can be done in various ways, leading to several possible three-dimensional structures: fcc, HCP, and RCP were the alternatives selected for detailed study.

Since the colloid consisted of spheres with a low refractive index contrast with respect to the surrounding solvent,

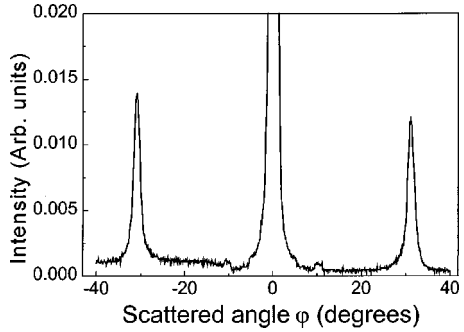

FIG. 5. Experimental data showing the intensity of the scattered light as a function of the scattering angle φ from the colloidal crystal measured from the zero-order transmitted beam. The peaks at $\pm 32.8°$ correspond to two of the Bragg spots. The relative intensity of each spot is obtained by calculating the area under each peak and is shown as a function of the angle of incidence θ in Fig. 6.

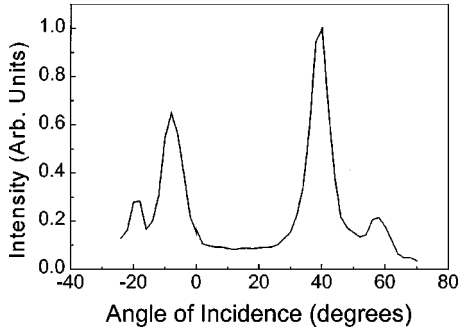

FIG. 6. The relative intensity of one of the Bragg spots as a function of the incident angle θ. Note the existence of four maxima of differing intensity. This compares well to the theoretical dependence of a twinned fcc structure shown in Fig. 8 which is calculated from simple scattering theory. Also note that the heights of the two main peaks are not the same, indicating that there are more layers of one type of fcc stacking than the other present in the crystal.

the strength of scattering from individual spheres is expected to be weak (for PMMA the refractive index is 1.49, and for octanol it is 1.43). The samples are also thin so that a single-scattering approximation should be valid. The intensity scattered from a plane parallel incident wave into a given direction was calculated by simply summing the scattered amplitudes from each of the spheres in the sample. The scattered amplitude from each sphere was calculated from exact Mie scattering theory. The effect of this is simply to multiply the intensity scattered from a point source by a form factor dependent on the angle between incident and scattered angles.

The summation of scattering amplitudes was performed in two stages. Each layer in the sample is assumed to consist of a perfect two-dimensional hexagonal structure of infinite extent, with the spheres in contact with six nearest neighbors. The scattering from this layer is calculated analytically—the results are the same as for a two-dimensional diffraction grating. The intensity is zero except for a discrete set of

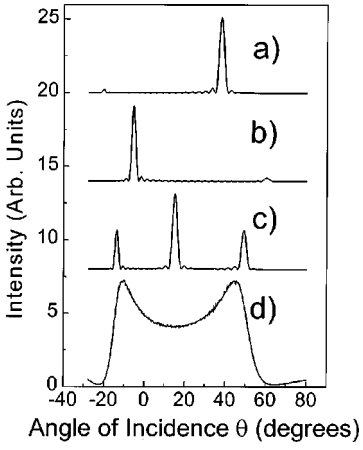

FIG. 7. The theoretical scattered intensity of one of the Bragg spots as a function of the angle of incidence for (a) a pure fcc structure with a stacking sequence ABCABCABC, (b) a pure fcc structure with a stacking sequence ACBACBACB, (c) HCP (ABABABABA-type stacking) and (d) RCP. All plots are for 20 layers of colloid suspended between two glass plates. They have been scaled and offset for clarity.

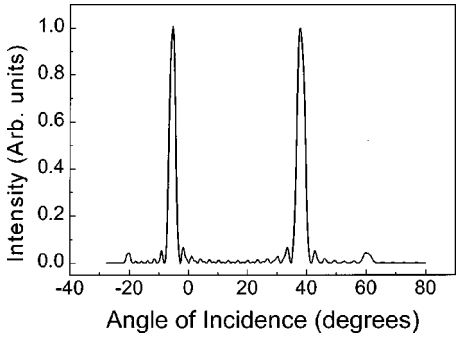

FIG. 8. The theoretical scattered intensity of one of the Bragg spots as a function of the angle of incidence for a twinned fcc structure based on ten layers of ABCABCABC-type stacking and ten layers of ACBACBACB-type stacking.

scattering angles dependent on the wavelength and the incident direction. The intensity in each of these directions is simply given by the Mie form factor mentioned above. The phase is a function of the incident and scattered angles, together with a term representing the phase of the grating—this is determined by the coordinates of any one sphere within the layer. The second stage is the summation over the number of layers in the sample, which was done numerically. For each of the structures of interest, a set of coordinates for one sphere in each of the layers was generated. This allowed the complex amplitudes scattered from each layer to be determined and then summed, giving the total amplitude and intensity scattered into a given direction from the structure of interest.

This approach is straightforward in the case of the HCP structure, for which the diffraction pattern depends only on the orientation of any one of the layers in the sample. In the case of the fcc structure, the two possible stacking sequences give rise to two structures differing by a rotation of 180°. This means that the six lowest-order Bragg spots, which are equivalent when a single layer is illuminated at normal incidence, become different for the fcc structure. In general, three high-intensity spots alternate with three low-intensity spots. A change to the other stacking sequence will exchange the roles of the two sets of spots. Another possibility, which is actually observed experimentally, is that both stacking sequences coexist in the same sample as twinned fcc, and if there are equal quantities of each of the two possible structures, then six equal-intensity Bragg spots are observed. To model this structure we simply sum the intensities produced by each of the two possible fcc orientations.

In the case of RCP we do not have a unique structure, but instead a statistical ensemble of alternative structures with equal probabilities. To model this, a Monte Carlo technique is used. A large number of alternative structures are generated, the diffraction from each is calculated, and the average intensity produced by all of them determined. We present the results from such calculations in Figs. 7 and 8, and note that the only structure which compares well to experiment is that of the twinned fcc.

DISCUSSION

Figures 9(a) and 9(b) show scanning electron microscope images of a shear-aligned colloidal crystal. To obtain this

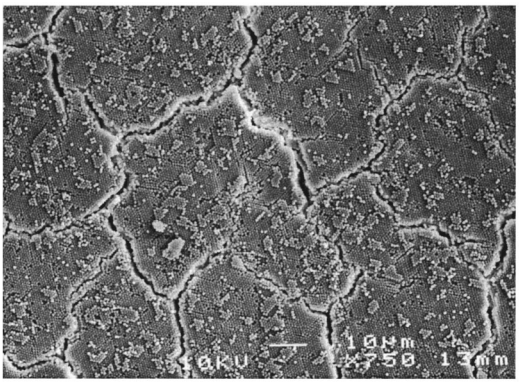

(a)

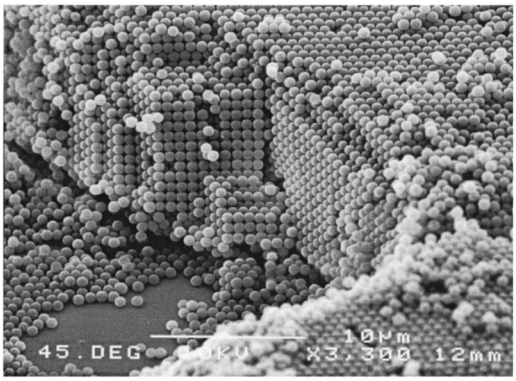

(b)

FIG. 9. (a) A scanning electron microscope image of a shear-aligned colloidal crystal produced from 790-nm-diameter PMMA spheres suspended in octanol. In order to image the crystal the top glass slide was removed. As a result the octanol evaporated causing some disorder of the structure due to shrinking. The cracked domains are about 50 μm in size. (b) Higher magnification of one of the domains clearly showing the ordering of the spheres within the crystal. In this case the ordering appears to be fcc.

image the top plate was carefully removed and the octanol allowed to evaporate. The resulting crystal consequently reduced in size and cracked into 50 μm size domains. However, higher magnification of one of the domains clearly shows hexagonal layering throughout the thickness of the crystal and in this particular case the structure appears to be fcc.

The intensity dependence of the Bragg spots shown in Fig. 6 compares well to that generated from weak scattering theory Fig. 8. The positions of the four main peaks show good agreement. However, the relative heights of the peaks clearly do not. The theoretical dependence assumes equal amounts of both types of fcc and is for a perfect crystal with no defects. The heights of the two main peaks in the experimental data are not equal indicating that there is more of one type of fcc than the other present in the sample (we estimate 60% of one type and 40% of the other based on the relative heights of the peaks). Also the widths of the peaks are greater than that predicted from theory. This is probably due to scattering from defects within the crystal. Work is currently in progress to examine more closely the defect type and density in shear-aligned colloidal crystals.

Figure 10 shows the transmission of two shear-aligned crystals of 10 and 115 μm thickness. The reduction in transmission at 1941 nm is due to the partial band gap. As expected, the reduction in transmission is larger for the thickest colloidal crystal due to the increased number of lattice planes giving rise to the reflection. At wavelengths outside the partial band gap there is little difference in transmission indicating similar scattering and absorption properties. It should also be noted that the transmission is high, around 80%; a useful property for many potential applications such as optical limiting and optical switching [34,37]. The transmission could be increased further if an antireflection coated slide were used instead.

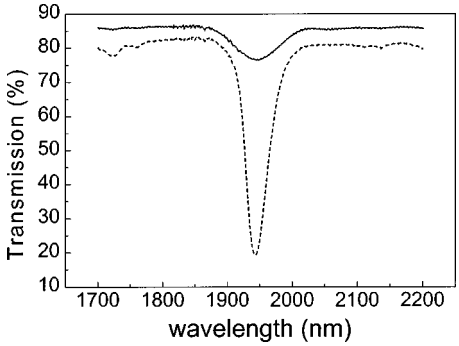

FIG. 10. The transmission at normal incidence as a function of wavelength for a 10-μm-thick (solid) and a 115-μm-thick (dotted) PMMA-octanol colloidal crystal. The first-order band gap is evident as a reduction in transmission at 1941 nm.

CONCLUSION

We have described a method to fabricate large-area colloidal crystals by inducing shear ordering during crystallization. The crystal structure has been controlled by careful shearing in one direction to form a single large-area fcc crystal, though with the present experimental configuration relaxation to a twinned fcc structure occurs over a period of minutes when the shearing force is removed. We have optically characterized the crystal structure by measuring the intensity of the Bragg spots as a function of the incidence angle and compared results to a simple weak scattering theory.

The shearing technique is a mechanical process and should be applicable to a variety of colloidal systems. We are currently studying other colloidal systems to verify the generality of the technique. Further, the cell geometry lends itself naturally to the fabrication of large-area thin colloidal crystals suitable for a range of applications—particularly optical limiting, optical switching, and optical routing [36,37]. It will be interesting to introduce a fluorescent species into the crystal to study how the modification of the density of optical modes within the crystal affects the spontaneous emission rate [38,39]. Further, we should like to fabricate crystals possessing the inverse fcc structure with a larger refractive index contrast in pursuit of a full photonic band gap.

ACKNOWLEDGMENTS

We thank Professor Peter Pusey and Dr. Andrew Schofield for useful conversations and for supplying us with the stabilized PMMA colloid.

[1] E. Yablonovitch, Phys. Rev. Lett. **58**, 2059 (1987).
[2] S. John, Phys. Rev. Lett. **58**, 2486 (1987).
[3] E. M. Purcell, Phys. Rev. **69**, 681 (1941).
[4] Y. H. Lee, Electron. Lett. **25**, 1377 (1989).
[5] N. W. Ashcroft and N. D. Mermin, *Solid State Physics* (Saunders, Philadelphia, 1979).
[6] R. F. Cregan, B. J. Mangan, J. C. Knight, T. A. Birks, P. St. J. Russell, P. J. Roberts, and D. C. Allan, Science **285**, 1537 (1999).
[7] V. N. Bogomolov *et al.*, Phys. Rev. E **55**, 7619 (1997).
[8] Yu. A. Vlasov, V. N. Astratov, O. Z. Karimov, A. A. Kaplyanskii, V. N. Bogomolov, and A. V. Prokofiev, Phys. Rev. B **55**, R13 357 (1997).
[9] V. N. Bogomolov, S. V. Gaponenko, A. M. Kapitonov, A. V. Prokefiev, A. N. Ponyavina, N. I. Silvanovich, and S. M. Samoilovich, Appl. Phys. A: Mater. Sci. Process. **63**, 613 (1996).
[10] V. N. Astratov, Yu. A. Vlasov, O. Z. Karimov, A. A. Kaplyanskii, Yu. G. Musikhin, N. A. Bert, V. N. Bogomolov, and A. V. Prokofiev, Phys. Lett. A **222**, (1996).
[11] S. Y. Lin, J. G. Fleming, M. M. Sigalas, R. Biswas, and K. M. Ho, Phys. Rev. B **59**, R15 579 (1999).
[12] R. Denning (private communication).
[13] N. A. Clark, A. J. Hurd, and B. J. Ackerson, Nature (London) **281**, 57 (1979).
[14] P. N. Pusey and W. van Megen, Nature (London) **320**, 340 (1986).
[15] P. N. Pusey and W. van Megen, Phys. Rev. Lett. **59**, 2083 (1987).
[16] W. L. Vos, M. Megans, C. M. van Kats, and P. Böseke, Langmuir **13**, 6004 (1997); **13**, 6120 (1997).
[17] P. A. Rundquist, P. Photinos, S. Jagannathan, and S. A. Asher, J. Chem. Phys. **91**, 4932 (1989).
[18] R. D. Pradhan, J. A. Bloodgood, and G. H. Watson, Phys. Rev. B **55**, 9503 (1997).
[19] A. Blanco, C. Lopez, R. Mayoral, H. Miguez, F. Meseguer, A. Mifsud, and J. Herrero, Appl. Phys. Lett. **73**, 1781 (1998).
[20] S. G. Romanov, A. V. Fokin, V. I. Alperovich, N. P. Johnson, and R. M. De La Rue, Phys. Status Solidi A **164**, 169 (1997).
[21] A. M. Kapitonov, N. V. Gaponenko, V. N. Bogomolov, A. V. Prokofiev, S. M. Samoilovich, and S. V. Gapanenko, Phys. Status Solidi A **165**, 119 (1998).
[22] A. A. Zakhidov, R. H. Baughman, Z. Iqbal, C. Cui, I. Khayrullin, S. O. Dantes, J. Marti, and V. G. Ralchenko, Science **282**, 897 (1998).
[23] J. E. G. J. Wijnhoven and W. L. Vos, Science **281**, 802 (1998).
[24] A. van Blaaderen, R. Ruel, and P. Wiltzius, Nature (London) **385**, 321 (1997).
[25] P. N. Pusey, W. van Megan, P. Bartlett, B. J. Ackerson, J. G. Rarity, and S. M. Underwood, Phys. Rev. Lett. **63**, 2753 (1989).
[26] C. Dux and H. Versmold, Phys. Rev. Lett. **78**, 1811 (1997).
[27] B. J. Ackerson and N. A. Clark, Phys. Rev. A **30**, 906 (1984).
[28] J. X. Zhu, M. Li, S. E. Phan, W. B. Russel, P. M. Chaikin, R. Rogers, and M. Meyer, in *Third Microgravity Fluid Physics Conference* (NASA Lewis Research Center, Cleveland, 1996), p. 397.
[29] J. Zhu, M. Li, R. Rogers, W. Meyer, R. H. Ottewill, W. B. Russel, and P. M. Chaikin, Nature (London) **387**, 883 (1997).
[30] T. M. Slawecki, C. J. Glinda, and B. Hammouda, Phys. Rev. E **58**, R4084 (1998).
[31] M. D. Haw, W. C. K. Poon, and P. N. Pusey, Phys. Rev. E **57**, 6859 (1998).
[32] M. D. Haw, W. C. K. Poon, and P. N. Pusey, Phys. Rev. E **58**, 4673 (1998).
[33] S. H. Park and Y. Xia, Adv. Mater. **10**, 1045 (1998).
[34] S. H. Park and Y. Xia, Langmuir **15**, 266 (1999).
[35] S. H. Park, D. Qin, and Y. Xia, Adv. Mater. **10**, 1028 (1998).
[36] L. Antl, J. W. Goodwin, R. D. Hill, R. H. Ottewill, S. M. Owens, S. Papworth, and J. A. Waters, Colloids Surface **17**, 67 (1986).
[37] P. L. Flaugh, S. E. O'Donnell, and S. A. Asher, Appl. Spectrosc. **38**, 847 (1984).
[38] E. P. Petrov, V. N. Bogomolov, I. I. Kalosha, and S. V. Gaponenko, Phys. Rev. Lett. **81**, 77 (1998).
[39] T. Yamasaki and T. Tsutsui, Appl. Phys. Lett. **72**, 1957 (1998).